Journal of Applied Polymer Science

Boron nitride based polyaniline nanocomposite: Preparation, property, and application

Sharique Ahmad,[1] Adil Sultan,[1] Waseem Raza,[2] M. Muneer,[2] Faiz Mohammad[1]

[1]Department of Applied Chemistry, Faculty of Engineering and Technology, Aligarh Muslim University, Aligarh 202002, India

[2]Department of Chemistry, Faculty of Science, Aligarh Muslim University, Aligarh 202002, India

Correspondence to: F. Mohammad (E-mail: faizmohammad54@rediffmail.com)

ABSTRACT: In this study, we report first time the electrical properties and photocatalytic activity of HCl doped polyaniline (Pani) and Pani/boron nitride (Pani/BN) nanocomposite prepared by *in situ* polymerization of aniline using potassium persulfate ($K_2S_2O_8$) in the presence of hexagonal boron nitride (h-BN). The prepared Pani and Pani/BN nanocomposite were characterized by Fourier transform infrared, X-ray diffraction, Thermogravimetric analysis, Scanning electron microscope, and Transmission electron microscope. The stability of the Pani/BN nanocomposite in comparison of Pani in terms of the DC electrical conductivity retention was investigated under isothermal and cyclic aging conditions. The Pani/BN nanocomposite in terms of DC electrical conductivity was observed to be comparatively more thermally stable than Pani. The degradation of Methylene blue (MB) and Rhodamine B (RhB) under UV-light irradiation were 50 and 56.4%, respectively, over Pani and 65.7 and 71.6%, respectively, over Pani/BN. The results indicated that the extent of degradation of MB and RhB was greater over nanocomposite material than Pani, which may result due to high electron–hole pairs charge separation under UV light. © 2016 Wiley Periodicals, Inc. J. Appl. Polym. Sci. **2016**, *133*, 43989.

KEYWORDS: catalysts; composites; conducting polymers

Received 4 February 2016; accepted 25 May 2016

DOI: 10.1002/app.43989

INTRODUCTION

Since the discovery of the first conducting polymer (polythiazyl),[1] such polymers have generated humongous interest due to their unique properties such as thermal stability, photocatalytic activity, electrical conductivity, etc.[2] These properties of conducting polymers furnished excellent potential for their applications in various fields such as in the manufacturing of cheap electronic devices,[3–5] television and other audio-video equipments[6,7] Polyaniline (Pani) is the most studied polymer among the different types of conducting polymers because of its easy synthesis, low cost of monomer, exclusive chemical properties and excellent environmental stability.[8–10] Moreover, it exists in three oxidation states leucoemeraldine, pernigraniline, and emeraldine. Among these, emeraldine salt form has highest conductivity[11] in the order of 1 S cm^{-1} and can be used in various applications due to reversible doping (conductive) and dedoping (nonconductive) mechanism such as in chemical and biological sensors[12–15] and actuators[16] etc. Hexagonal boron nitride (h-BN), a structural analogue of graphite having good thermal transport properties.[17,18] Among all other BNs, h-BN is the most preferred polymorph in which boron and nitrogen atoms form planar conjugated layers.[19] BNs have various unique properties such as hardness, thermal stability, high melting point, good corrosion resistance, good dielectric breakdown strength, resistance to oxidation, and chemical inertness. There are many applications, for example, optical storage, medical treatment, photocatalytic reactions, and electrical insulation[20,21] in which BNs used. Wang *et al.* reported[22] that h-BN/SnO_2 material showed good photocatalytic activity was mainly due to its suitable band gap energy, strong adsorption ability for methyl orange, and effective charge separation at the h-BN/SnO_2 photocatalyst interface. Sadia *et al.*[23] synthesized the Pani/graphene nanocomposite that delivered a significant degradation of RB (rose Bengal) dye by ~56% within 3 h under UV–vis light. They observed that the heterojunctions are formed in the space charge separation region at the Pani/graphene interfaces and suggested that graphene may accept the photoexcited electrons from Pani. Similarly to graphene, h-BN may be a promising material of photocatalytic nanocomposite with Pani. To the best of our knowledge, the photocatalytic degradation of RhB and MB dyes over the surface of Pani/BN nanocomposite as photocatalyst has not been reported elsewhere. Herein, we have tried to look forward our effort for enhancement of photocatalytic activity of Pani by using BN under UV-light. The h-BN nanosheets have large surface area, which may have significantly increased the adsorption of dyes and photoinduced charge

transfer along the h-BN sheets in nanocomposite. A conducting nanocomposite of Pani with h-BN (Pani/BN) was prepared via *in situ* polymerization method. The photocatalytic degradation of MB and RhB dyes have been studied over the surface of the prepared Pani/BN nanocomposite which efficiently degraded both of the dyes by 65.7% (MB) and 71.6% (RhB). The structure and surface morphology were investigated. The thermal stability was also investigated in terms of DC electrical conductivity retention under isothermal and cyclic accelerated aging conditions.

EXPERIMENTAL

Materials

In the preparation of Pani and Pani/BN nanocomposite the main chemicals used were aniline, 99% (E.Merck, India), hydrochloric acid, 35% (E. Merck, India), h-BN (MK Nano, Canada), potassium persulfate (E.Merck, India) and methanol. Double distilled water was used throughout the experiments.

Preparation of Pani and Pani/BN Nanocomposite

The nanocomposite of Pani/BN was prepared by *in situ* oxidative polymerization of aniline in the presence of h-BN using potassium persulfate as an oxidizing agent. At first 10 wt % h-BN was ultrasonicated for 3 h in 100 mL of 1 *M* HCl then it was added to aniline solution dropwise under constant stirring for 1 h to enable the proper dispersion of h-BN in aniline. Oxidant solution was then added dropwise in the above dispersed solution of h-BN and aniline to polymerize the aniline. As the oxidant, was added the color of the reaction mixture starts changing from light purple to dark green within 20 min of stirring. The stirring was kept continuous for 20 h. The final dark green colored reaction mixture was then filtered, washed with double distilled water and methanol to remove excess acid, potassium persulfate, and Pani oligomers until filtrate became colorless and neutral. Thus prepared Pani/BN nanocomposite was dried at 80 °C for 12 h in an air oven, crushed into fine powder and was stored in desiccator for further investigations. Pani was also prepared using the same method as described above in absence of h-BN. The as prepared materials were designated as Pani and Pani/BN.

Photodegradation Experiment

The photocatalytic oxidation of Rhodamine B (RhB) and Methylene Blue (MB) solution was done under UV-light illumination to evaluate the photocatalytic activity of the Pani and Pani/h-BN nanocomposite under constant stirring and bubbling of atmospheric oxygen. An immersion well photochemical reactor made of Pyrex glass with a 250 mL working volume of dyes equipped with magnetic stirring bar and an opening for supply of molecular oxygen was used for all the experiments. A 125-W medium pressure mercury lamp was used as the UV-light source. During all the experiments, the temperature of aqueous solutions of dyes was maintain $\sim 20 \pm 0.5$ °C by refrigerated water circulation to prevent the heating of the solutions by radiations emitted by the UV-lamp (IR and short wave length). The radiation intensity falling on the solutions was measured using UV light intensity detector (Lutron UV-340) and found to be 3.22 mW/cm^2. Typically, 250 mg Pani and Pani/h-BN nanocomposite was added into 250 mL aqueous solution of RhB (8 ppm) and MB (10 ppm), respectively. The solution was continuously stirred in the dark for 30 min to ensure the establishment of adsorption−desorption equilibrium between the photocatalyst and the dyes prior to irradiation.[24] Then the solution was exposed to UV light. During irradiation, sample was withdrawn from reactor using a syringe at regular intervals and centrifuged before the measurement to remove the powder photocatalyst. The decolorization of dye was measured by using UV–vis spectrophotometer (Perkin Elmer $\lambda = 35$) at the $\lambda_{max} = 553$ and 663, respectively, based on Beer Lambert Law.[25] The degradation efficiency of dyes was calculated by using eq. (1).

$$\text{Degradation } \% = A_0 - A_t / A_0 \times 100\% \quad (1)$$

where A_0 and A_t are the concentrations of sample at time "0" and time "*t*."

CHARACTERIZATIONS

The Fourier transform infrared spectroscopy (FTIR) spectra were recorded using Perkin-Elmer 1725 instrument. X-ray diffraction (XRD) pattern were recorded by Bruker D8 diffractometer with Cu Ka radiation at 1.540 A°. Scanning electron microscope (SEM) studies were carried out by JEOL, JSM, 6510-LV (Japan). Transmission electron microscope (TEM) studies were carried out by using JEM 2100, JEOL (Japan). Thermogravimetric analysis (TGA) was done by using a Perkin Elmer instrument in the temperature range from 35 to 800 °C. The thermal stability of Pani and Pani/BN nanocomposite under isothermal and cyclic ageing conditions was studied in terms of DC electrical conductivity retention. For this study a four-in-line probe with a temperature controller, PID-200 (Scientific Equipments, Roorkee, India) was used to measure the DC electrical conductivity and its temperature dependence. The equation used in calculation of DC electrical conductivity was

$$\sigma = [\ln 2(2S/W)]/[2\pi S(V/I)] \quad (2)$$

where *I*, *V*, *W*, and *S* are the current (A), voltage (V), thickness of the pellet (cm), and probe spacing (cm) respectively and σ is the conductivity (S/cm).[2] In testing of isothermal stability, the pellets were heated at 50, 70, 90, 110, and 130 °C in an air oven and the DC electrical conductivity was measured at particular temperature at an interval of 10 min in the accelerated ageing experiments. In testing of the stability under cyclic ageing condition, DC conductivity measurements were taken five times at an interval of about 90 min within the temperature range of 50–150 °C.

RESULTS AND DISCUSSION

Mechanism of Preparation of Pani and Pani/BN Nanocomposite

The mechanistic view of the polymerization process seems to involve the anilinium cations (phenyl-NH_3^+) getting hooked up by Coulombic attraction between anilinium cations and the surface of h-BN. Thus the h-BN gets completely surrounded by anilinium cations. This arrangement comes in contact with $K_2S_2O_8$, the anilinium cations get polymerized on the surface of h-BN forming Pani (emeraldine salt). h-BN has partially polar bonds,[26] which may cause interaction with polarons and lone pairs of Pani, as mentioned in our previous work with

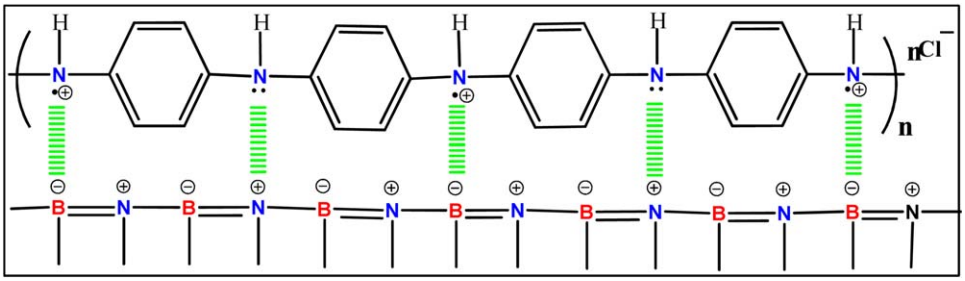

Figure 1. Schematic presentation of Coulombic attraction between Pani and h-BN in Pani/BN nanocomposite. [Color figure can be viewed in the online issue, which is available at wileyonlinelibrary.com.]

polypyrrole/BN nanocomposite.[27] The Pani (emeraldine salt) formed on the surface of h-BN get attached by Coulombic attraction between the positive charge on nitrogen of Pani and negative charge on boron of h-BN and also the interaction between lone pair of nitrogen of Pani (emeraldine salt) and positive charge on nitrogen of h-BN. Schematic presentation of coulombic attraction between the +ve and −ve charges is given in Figure 1.

FTIR Spectroscopic Study

FTIR spectra of the Pani/BN nanocomposite and Pani are shown in Figure 2. The characteristic peak of Pani at 3434 cm^{-1} corresponds to N—H stretching vibration. The peak at 1571 and 1489 cm^{-1} is due to C=C stretching mode of the quinoid and benzenoid rings, respectively, and the peak at about 1287 cm^{-1} can be assigned to C—N stretching. The peak at 790 cm^{-1} is usually assigned to an out-of-plane bending vibration of C—H, which confirmed the formation of Pani.[28] In the Pani/BN nanocomposite, there are the two more peaks situated at 1375 and 792 cm^{-1}, respectively. The absorption band at 1375 cm^{-1} can be attributed to the in-plane B-N stretching, and the absorption band at 792 cm^{-1} belongs to the B–N–B out-of-plane bending vibration which is assumed to overlap with C—H out of plane bending vibration.[29] While the remaining peaks are similar to that of Pani but slightly shifted to higher wavenumber with reduced intensity indicative of strong interaction between Pani and h-BN.

XRD Studies

The XRD patterns of Pani and Pani/BN nanocomposite are shown in Figure 3. Figure 3(b) shows the broad peak at $2\theta = 25.29°$ may be attributed to Pani. In the Figure 3(a) shows XRD pattern of Pani/H-BN nanocomposite, a sharp peak observed at $2\theta = 25.78°$, which suggested that the interaction between h-BN and Pani. In Pani/BN nanocomposite, highly crystalline nature of h-BN and amorphous nature of Pani has been merged and shifted from 25.29°. The other peaks around at $2\theta = 40.23°$, 42.83°, and 49.25° in the pattern of Pani/BN may be attributed to h-BN.[30]

Thermogravimetric Analysis

Figure 4 represents the TGA thermograms of Pani and Pani/BN nanocomposite, which shows the three step weight loss process. In the case of Pani, there are three major stages of weight loss; first around 120 °C, second in range from 130 to 400 °C and third in range from 400 to 550 °C due to the loss of water, removal lower oligomers of Pani and thermo-oxidative decomposition of Pani, respectively.[31] It is found that the degradation of nanocomposite is quite similar to that of Pani. The observable difference is the higher thermal stability of Pani/BN nanocomposite. The decomposition of Pani/BN started at around

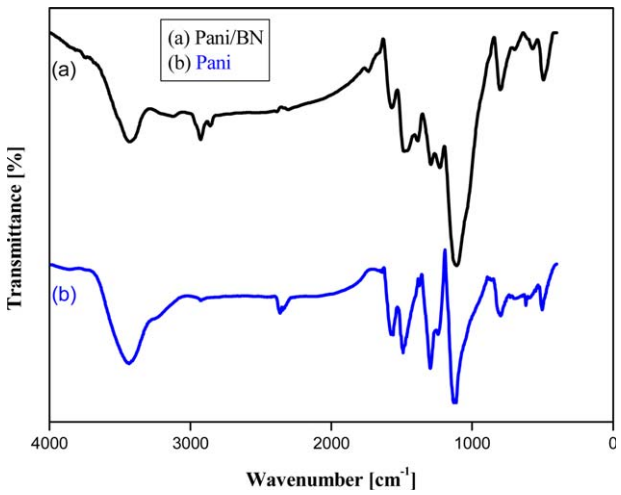

Figure 2. FTIR spectra of: (a) Pani/BN nanocomposite and (b) Pani. [Color figure can be viewed in the online issue, which is available at wileyonlinelibrary.com.]

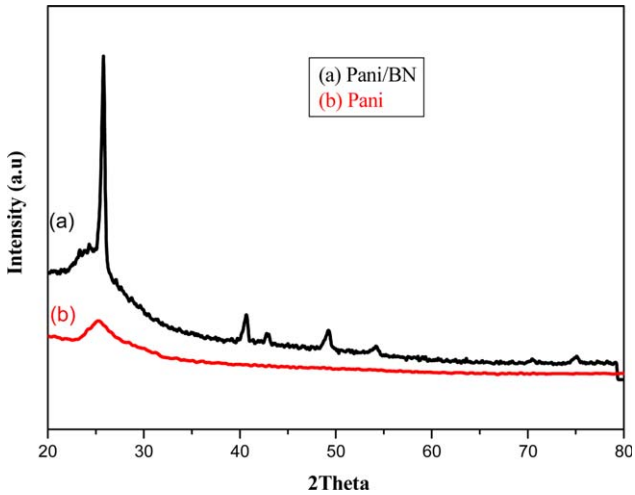

Figure 3. XRD patterns of: (a) Pani/BN nanocomposite and (b) Pani. [Color figure can be viewed in the online issue, which is available at wileyonlinelibrary.com.]

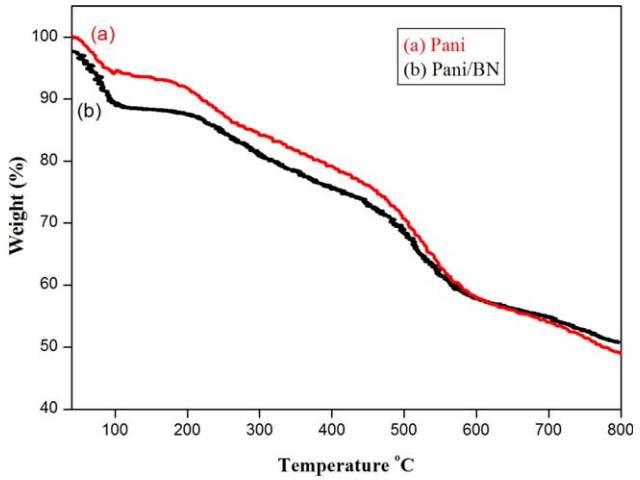

Figure 4. TGA thermograms of: (a) Pani and (b) Pani/BN nanocomposite. [Color figure can be viewed in the online issue, which is available at wileyonlinelibrary.com.]

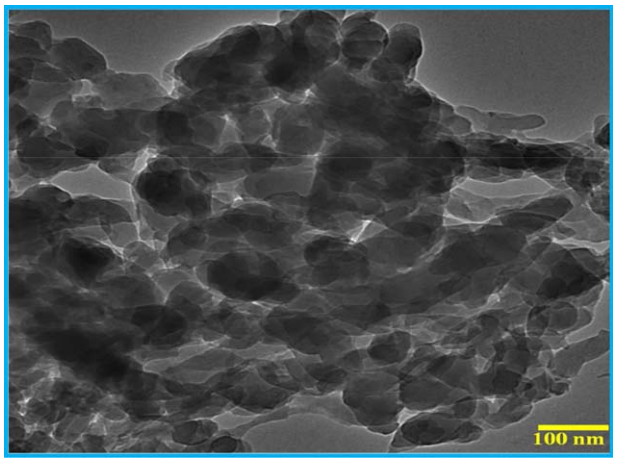

Figure 6. TEM micrograph of Pani/BN nanocomposite. [Color figure can be viewed in the online issue, which is available at wileyonlinelibrary.com.]

492 °C, which is at much higher temperature than in Pani (~475 °C). This enhanced stability may be due to high thermal stability of h-BN that has strong Coulombic attraction with Pani.

SEM Studies

The SEM of Pani and Pani/BN nanocomposite are shown in Figure 5 at different magnifications. The SEM micrograph in Figure 5(a) shows the sheet like structure of h-BN. In Figure 5(b) SEM image of Pani shows short tubes along with flakes like structure. The SEM images in Figure 5(c,d) represent the Pani/BN, in which the polymer matrix is well enwrapped on h-BN with uniform dispersion and some sheet like morphology may also be seen. This suggests that h-BN acted as sheet on which polymerization took place and facilitated in the formation of some sheet like structures.

TEM Studies

TEM micrograph of Pani/BN nanocomposite is shown in Figure 6. From the Figure, it is observed that the light gray sheet type structure seem to BN and dark gray seem to Pani, which is enwrapped on the BN nanosheets. Thus, it may be said that aniline underwent polymerization on the surface of h-BN giving the sheet type structure.

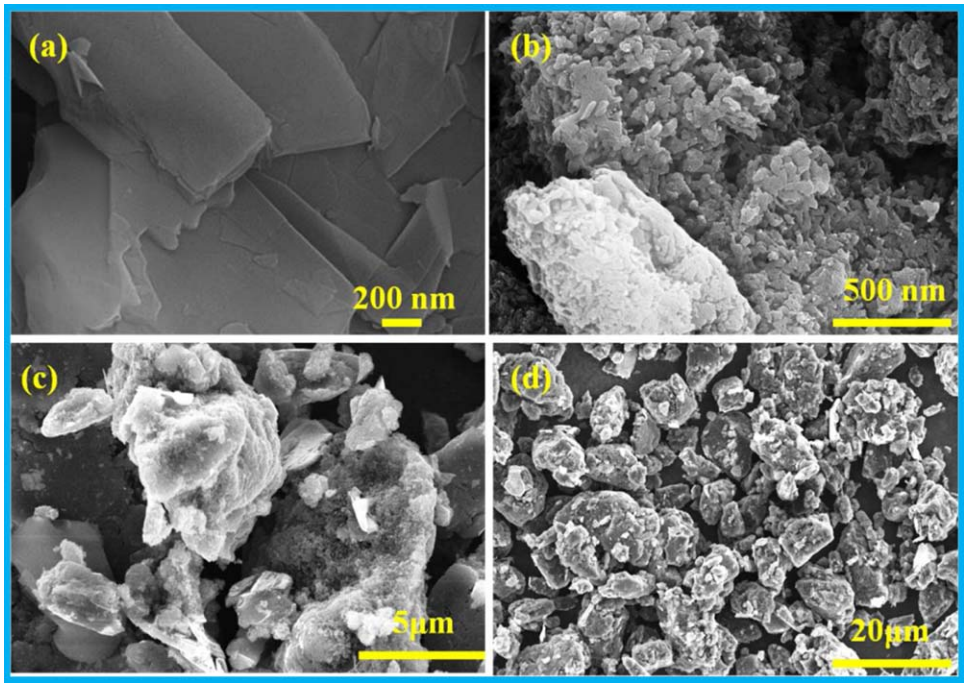

Figure 5. SEM micrographs of: (a) h-BN, (b) Pani, and (c,d) Pani/BN nanocomposite at different magnification. [Color figure can be viewed in the online issue, which is available at wileyonlinelibrary.com.]

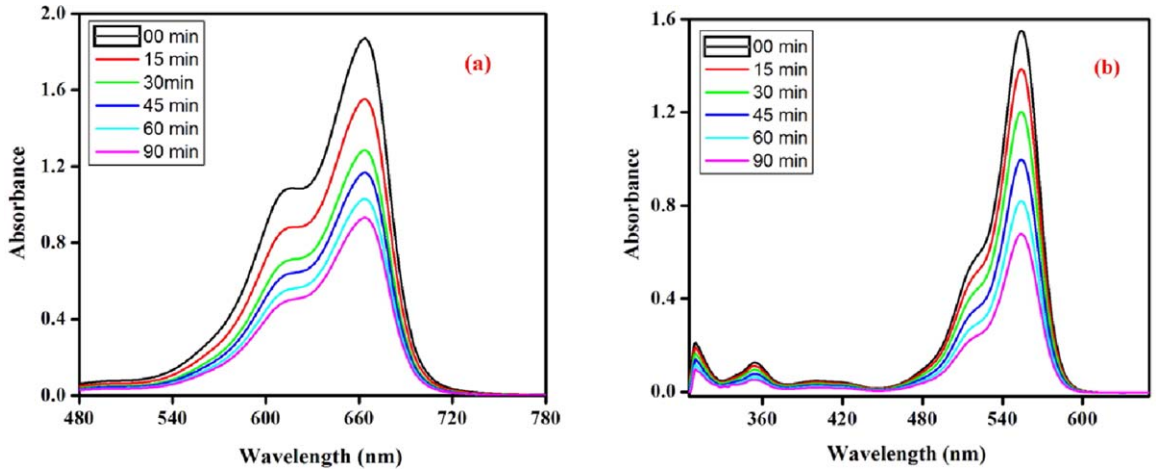

Figure 7. (a,b). Photocatalytic degradation of MB and RhB dyes, respectively, at different time intervals in the presence of Pani. [Color figure can be viewed in the online issue, which is available at wileyonlinelibrary.com.]

PHOTOCATALYTIC STUDIES

The photocatalytic activity of Pani and Pani/BN nanocomposite was investigated by the decolorization of RhB and MB in aqueous solution which is discarded by textile industries under UV-light illumination. The controlled experiment indicates that RhB and MB were resistant towards the degradation under UV-light irradiation without a photocatalyst. However, little decomposition of dyes takes place in the presence of prepared photocatalyst in dark due to adsorption of dyes on the surface of catalysts. The RhB showed good adsorption on the surface of synthesized photocatalyst. The result indicates that both light and catalyst were required for efficient photocatalytic degradation. The decomposition of the dyes was monitored by measuring the change in the absorbance at their (λ_{max} 663 and 553) as a function of irradiation time. Figure 7(a,b) showed that 50 and 56.4% decolorization of MB and RhB dyes take place, respectively, after 90 min of irradiation time over Pani. Figure 8(a,b) indicates the 65.7 and 71.1% degradation of MB and RhB, respectively, after 90 min as a function of irradiation time in the presence of Pani/BN nanocomposite material. The results of Figures 7 and 8 illustrate that the main peaks of both the dyes (553 and 663 nm) decreases gradually as irradiation time increase. The color of the dyes solution became lighter as the irradiation time increased due to gradually degradation of chromophoric groups present in the dyes.[32,33] The Figures 7 and 8 displayed the decolorization of MB was found to be lower than RhB due to presence of stable and bulky aromatic rings, which suppress the interaction between catalysts and dye.[34] The adsorption of MB was lower than RhB on the surface of catalyst which decrease photocatalytic degradation of MB. Figure 9 showed the percentage degradation of dyes under UV-light illumination over Pani and Pani/BN nanocomposite. It was found that the degradation of RhB was more than that of MB by hydroxyl radicals. It can be attributed due to absorption of less UV-light by RhB than MB.[35] Hence more photons were available to photocatalyst, which raised the formation of hydroxyl radicals. The degradation of both dyes was found to be higher over Pani/BN nanocomposite material than Pani. The Pani

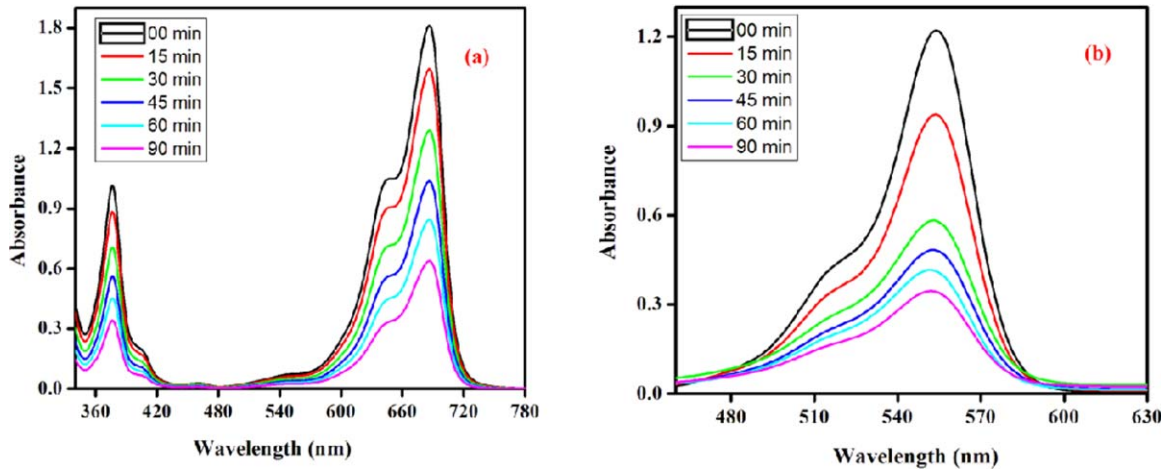

Figure 8. (a,b) Photocatalytic degradation of MB and RhB dyes, respectively, at different time intervals in the presence of Pani/BN nanocomposite. [Color figure can be viewed in the online issue, which is available at wileyonlinelibrary.com.]

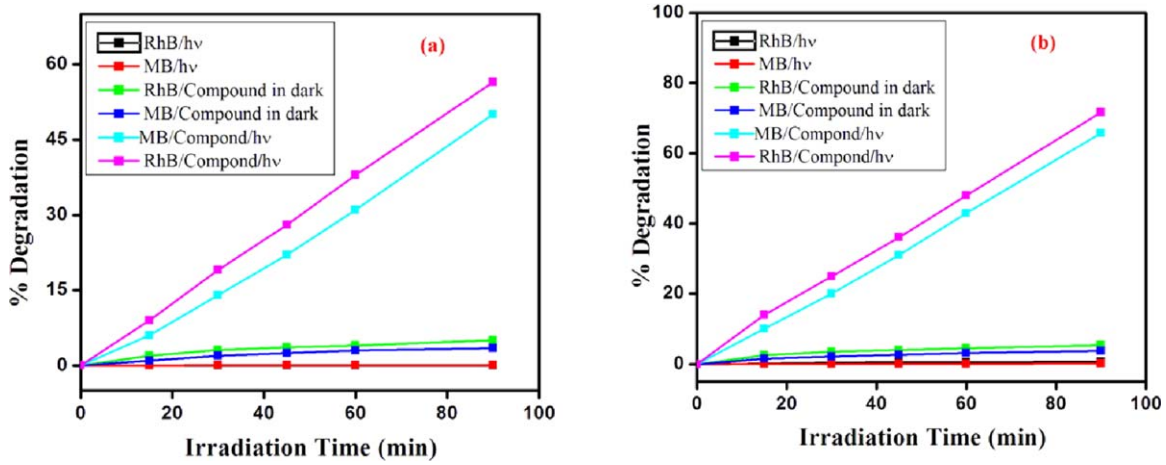

Figure 9. (a) Percentage degradation of MB and RhB dyes in aqueous solution as a function of time in the presence and absence of Pani and presence and absence of UV-light, (b) Percentage decomposition of both dyes in aqueous solution as a function of time in the presence and absence of Pani/BN and presence and absence of UV-light. [Color figure can be viewed in the online issue, which is available at wileyonlinelibrary.com.]

interacted with h-BN nanosheets that substantially increased the surface area of the nanocomposite, therefore more degradation of both dyes over the surface of Pani/BN nanocomposite than Pani. It may be also due to the electron transfer from excited Pani to h-BN and further across nanocomposite interface, which leads to formation of trapping sites by h-BN, which increase the charge separation by splitting the arrival time of photogenerated electron and hole to reach the surface of photocatalyst and thus decrease the electron-hole recombination rate.[36–38] The photocatalytic activity of Pani/BN nanocomposite was also investigated for waste water treatment by taking sewage from department of chemistry, Aligarh Muslim University, India. Figure 10 indicates 53% degradation of waste water after 90 min as a function of irradiation time in the presence of Pani/BN nanocomposite. Thus Pani/BN nanocomposite found to be a good photocatalyst also for waste water treatment.

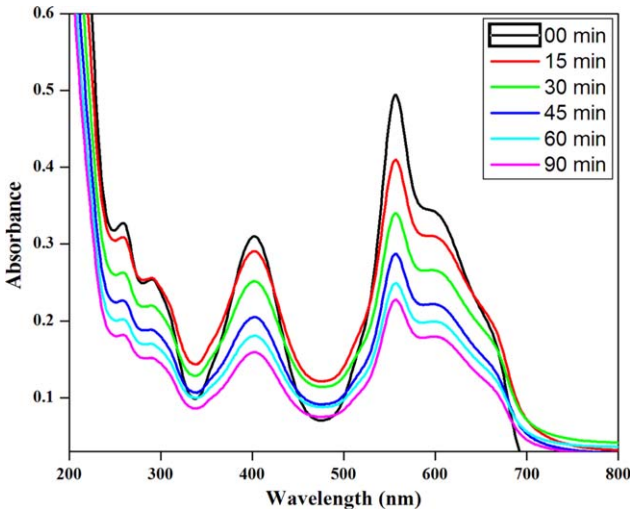

Figure 10. Photocatalytic treatment of waste water at different time intervals in the presence of Pani/BN nanocomposite. [Color figure can be viewed in the online issue, which is available at wileyonlinelibrary.com.]

Possible Mechanism

The possible mechanism for the degradation of dye using Pani/BN nanocomposite can schematically be represented in Figure 11. Pani is a typical semiconducting polymer with an extended π-electron conjugation system. Pani serves as a good photocatalyst for degradation of pollutants under UV light irradiation due to its electronic structure characterized by a filled valence band (HOMO) and an empty conduction band (LUMO). On absorption of photons that match or exceed the band gap energy of Pani, an electron may be promoted from the valence band to the conduction band leaving behind an electron vacancy or "hole" in the valence band.[39] In Pani/BN nanocomposite the charge separation is maintained by transferring of electrons from Pani to h-BN through nanocomposite interface which decreased the electrons and holes recombination. Thus electrons and holes can migrate to the catalyst surface where they participate in redox reactions with adsorbed dyes. Specially, the holes generated in the valence band (h^+_{VB}) can react with surface bound H_2O molecules to produce hydroxyl radicals and

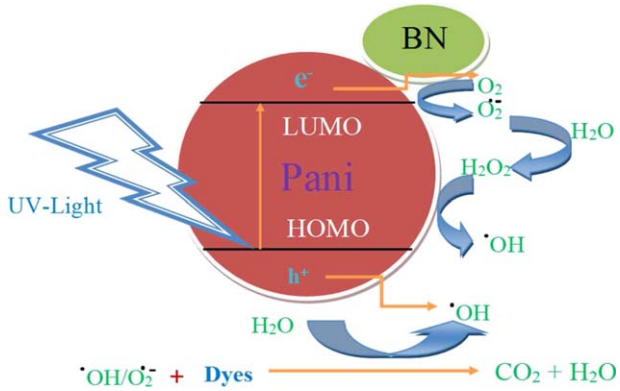

Figure 11. Schematic presentation of probable degradation process of MB and RhB over Pani/BN nanocomposite. [Color figure can be viewed in the online issue, which is available at wileyonlinelibrary.com.]

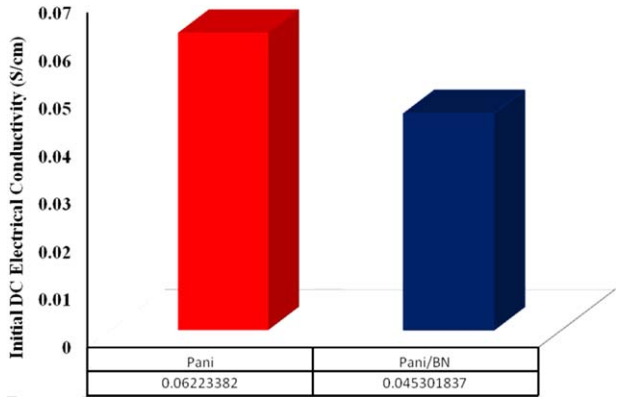

Figure 12. Initial DC electrical conductivity of (a) Pani and (b) Pani/BN. [Color figure can be viewed in the online issue, which is available at wileyonlinelibrary.com.]

the electrons present in the conduction band (e^-_{CB}) are picked up by oxygen to generate superoxide radical anions.[25,39]

$$\text{Pani/BN} \xrightarrow[\text{(UV-radiations)}]{} e^-_{CB} + h^+_{VB} \quad (3.1)$$

$$O_2 + e^-_{CB} \longrightarrow O_2^{\bullet -} \quad (3.2)$$

$$H_2O + h^+_{VB} \longrightarrow H^+ + {}^{\bullet}OH \quad (3.3)$$

$$O_2 + 2(e^-_{CB}) + 2H^+ \longrightarrow H_2O_2 \quad (3.4)$$

$$e^-_{CB} + O_2^{\bullet -} + 2H^+ \longrightarrow {}^{\bullet}OH + {}^{-}OH \quad (3.5)$$

The superoxide radical anions act as strong reducing agent and hydroxyl radical act as strong oxidizing agent and degrade the pollutant dyes to the mineral end products.

$$h^+_{VB} + \text{Dye} \longrightarrow \text{Degraded products} + H_2O + CO_2 \quad (3.6)$$

$${}^{\bullet}OH + \text{Dye} \longrightarrow \text{Degraded products} + H_2O + CO_2 \quad (3.7)$$

ELECTRICAL CONDUCTIVITY

The electrical conductivities of Pani and Pani/BN nanocomposite were measured by standard four-in-line probe method. From the measured electrical conductivity it may be inferred that both the as prepared materials are semiconducting in nature and the addition of h-BN to the Pani has a significant effect on its electrical conductivity. The measured electrical conductivities of Pani and Pani/BN nanocomposite were 0.0622 and 0.045 S/cm, respectively, as shown in Figure 12. Thus it is observed that the electrical conductivity decreased after loading of BN. The BN, having insulating behaviour may induce the formation of less efficient network for charge transport in the Pani chains leading to the less electrical conductivity than Pani. The reason for decrease in electrical conductivity of Pani/BN nanocomposite may also be due to interaction of boron (−ve charge) and nitrogen (+ve charge) atoms of h-BN with polarons/bipolarons of Pani as presented in Figure 1. This causes the loss of mobility of charge carriers leading to reduced electrical conductivity in Pani/BN nanocomposite.

Stability under Isothermal Ageing

The stability of Pani and Pani/BN nanocomposite in terms of DC electrical conductivity retention was studied under isothermal ageing conditions as shown in Figure 13. The representation of relative electrical conductivity was calculated by the equation:

$$\sigma = \frac{\sigma_f - \sigma_i}{t} \quad (4)$$

where σ is the change in relative electrical conductivity/minute, σ_f is the final relative electrical conductivity at temperature T, σ_i is the initial relative electrical conductivity at temperature T, and t is the duration of the experiment (40 min). The electrical conductivity was measured for each temperature (50, 70, 90, 110, and 130 °C) versus time. From the Figure 13(a), it can be

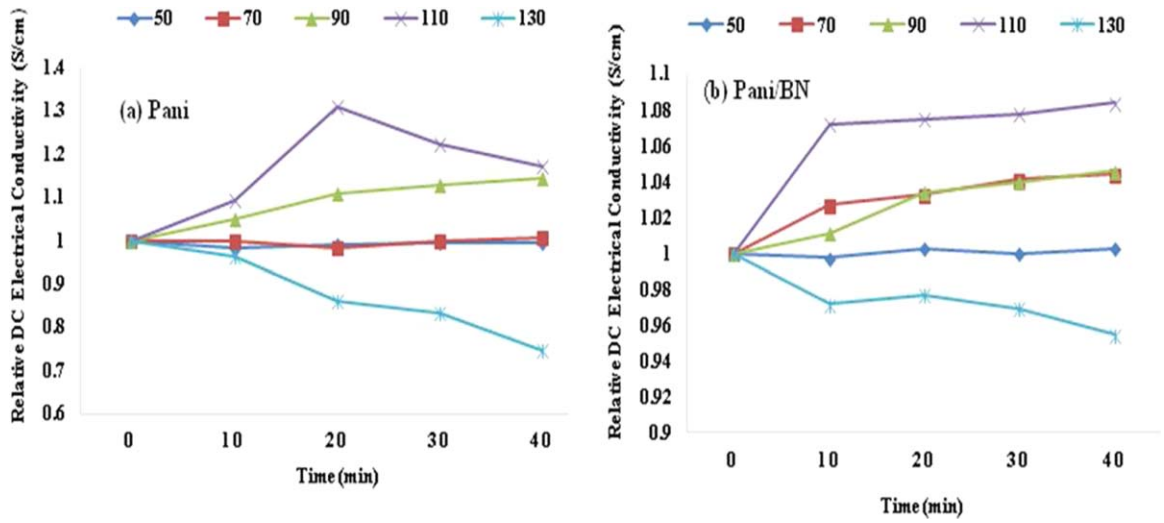

Figure 13. DC electrical conductivity retention under isothermal conditions at 50, 70, 90, 110, and 130 °C of (a) Pani and (b) Pani/BN. [Color figure can be viewed in the online issue, which is available at wileyonlinelibrary.com.]

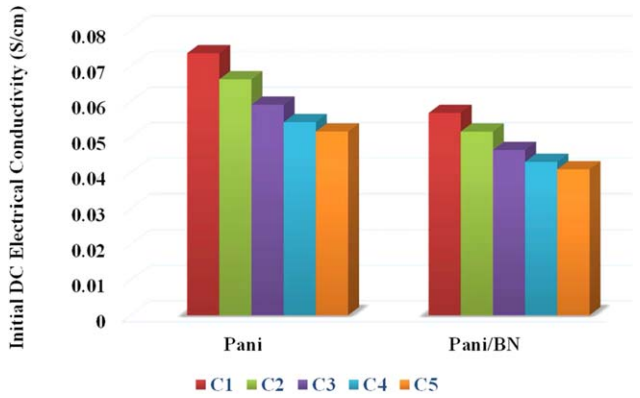

Figure 14. DC electrical conductivity at the start of each cycle of Pani and Pani/BN nanocomposite under cyclic ageing conditions. [Color figure can be viewed in the online issue, which is available at wileyonlinelibrary.com.]

understood that the stability of Pani is very fair at 50, 70, and 90 °C while the electrical conductivity becomes unstable at 110 and 130 °C. The Pani/BN nanocomposite is quite stable at 50 °C and also significantly stable at 70 and 90 °C as shown in Figure 13(b). The nanocomposite shows more instability as compared to Pani at 110 and 130 °C.

Stability under Cyclic Ageing Conditions

The stability of Pani and Pani/BN nanocomposite in terms of DC electrical conductivity was also studied by cyclic ageing technique. From the Figure 14, it may be observed that the initial DC electrical conductivity at the start of each cycle decreases with increase in cycle number for both Pani and Pani/BN nanocomposite. The difference in electrical conductivity of Pani and Pani/BN nanocomposite from cycle 1 to cycle 5 was observed 0.0221 and 0.0158 S/cm, respectively. Therefore Pani/BN nanocomposite is shown more stable than Pani.

The stability in the term DC electrical conductivity retention of Pani and Pani/BN nanocomposite was studied by cyclic ageing technique within the temperature range of 50 to 150 °C as shown in Figure 15. As the number of cycle increases, the DC

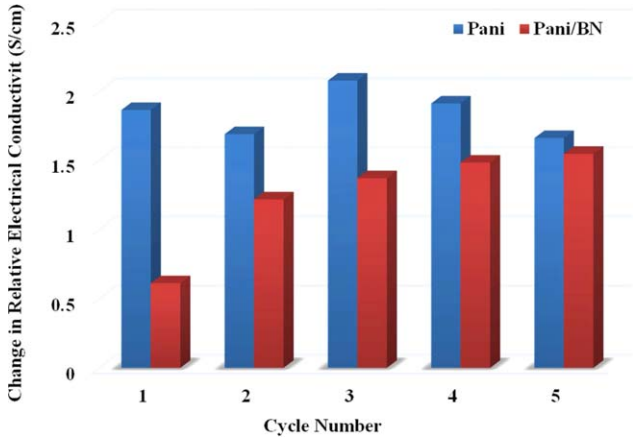

Figure 15. DC electrical conductivity retention under cyclic ageing conditions of Pani and Pani/BN nanocomposite. [Color figure can be viewed in the online issue, which is available at wileyonlinelibrary.com.]

electrical conductivity gain for Pani decreases but the change in electrical conductivity becomes less from cycle third to fifth. In case of Pani/BN nanocomposite, it is observed that there is only gain in the electrical conductivity from first cycle to fifth cycle. After second cycle, the gain in electrical conductivity of Pani/BN nanocomposite seems stable. From these observations, it may attributed that the Pani/BN has more stable electrical conductivity under cyclic ageing condition. The different pattern of conductivities in different cycles for Pani and Pani/BN nanocomposite may be attributed to the removal of moisture, excess of HCl or low molecular weight oligomers of aniline.[31]

CONCLUSIONS

Pani and Pani/BN nanocomposite were synthesized by *in situ* polymerization method and characterized by different instrumental techniques. The DC electrical conductivity retention under isothermal and cyclic ageing conditions has also been presented. It was observed that Pani showed greater electrical conductivity as well as isothermal stability than that of Pani/BN nanocomposite but in terms of cyclic stability Pani/BN showed good stability than that of Pani. The as prepared materials possessed the excellent photodecomposition of model dyes under UV-light irradiation. It was observed that photogenetrated hydroxyl radical and hole (h+) and superoxide ions were the main active species responsible for degradation of both the dyes. The results highlighted that the extent of degradation of MB and RhB was greater over Pani/BN nanocomposite than Pani. This indicates that the as prepared Pani/BN nanocomposite may be used as a photocatalyst even at high thermal conditions (≤90 °C) for waste water treatment.

ACKNOWLEDGMENTS

Sharique Ahmad gratefully acknowledges the Maulana Azad National Fellowship granted by University Grant Commission.

REFERENCES

1. Bardeen, J.; Cooper, L. N.; Schrieffer, J. R. *Phys. Rev.* **1957**, *106*, 162.
2. Ansari, M. O.; Mohammad, F. *Sens. Actuators B* **2011**, *157*, 122.
3. Huang, Z.; Wang, P. C.; MacDiarmid, A. G.; Xia, Y.; Whitesides, G. M. *Langmuir* **1997**, *13*, 6480.
4. Wang, J. Z.; Zheng, Z. H.; Li, H. W.; Huck, W. T. S.; Sirringshaus, H. *Synth. Met.* **2004**, *146*, 287.
5. Menard, E.; Meitl, M. A.; Sun, Y.; Park, J. U.; Shir, D. J. L.; Nam, Y. S.; Jeon, S.; Rogers, J. A. *Chem. Rev.* **2007**, *107*, 1117.
6. Gustafsson, G.; Cao, Y.; Trecay, G. M.; Klavetter, F.; Colaneri, N.; Heeger, A. *J. Nature* **1992**, *357*, 477.
7. Sugimoto, T.; Ono, K.; Ando, A.; Kurozumi, K.; Hara, A.; Morita, Y.; Miura, A. *Appl. Acoust.* **2009**, *70*, 1021.
8. Yang, C. Y.; Cao, Y.; Smith, P.; Heeger, A. J. *Synth. Met.* **1993**, *53*, 293.
9. Ikkala, O. T.; Laakso, J.; Väkiparta, K.; Virtanen, E.; Ruohonen, H.; Järvinen, H. *Synth. Met.* **1995**, *69*, 97.

10. Tiitu, M.; Talo, A.; For'sen, O.; Ikkala, O. *Polymer* **2005**, *46*, 6855.
11. Stejskal, J.; Gilbert, R. G. *Pure Appl. Chem.* **2002**, *74*, 857.
12. Hatchett, D. W.; Josowicz, M. *Chem. Rev.* **2008**, *108*, 746.
13. Haung, J.; Virji, V.; Weiller, B. H.; Kaner, R. B. *Chem. Eur. J.* **2004**, *10*, 1314.
14. Anil kumar, P.; Jayakannan, M. *Langmuir* **2008**, *24*, 9754.
15. Ma, Y.; Ali, S. R.; Dodoo, A. S.; He, H. *J. Phys. Chem. B* **2006**, *110*, 16359.
16. Yan, H.; Tomizawa, K.; Ohno, H.; Toshima, N. *Macromol. Mater. Eng.* **2003**, *288*, 578.
17. Golberg, D.; Bando, Y.; Huang, Y.; Terao, T.; Mitome, M.; Tang, C. C.; Zhi, C. Y. *ACS Nano* **2010**, *4*, 2979.
18. Lindsay, L.; Broido, D. A. *Phys. Rev. B* **2011**, *84*, 155421.
19. Lin, Y.; Williams, T. V.; Elsayed-Ali, H. E.; Connell, J. W. *J. Phys. Chem.* **2010**, *114*, 17434.
20. Shi, L.; Gu, Y.; Chen, L.; Qian, Y.; Yang, Z.; Maa, J. *J. Solid State Chem.* **2004**, *177*, 721.
21. Rudolph, S. *Interceram* **1993**, *42*, 302.
22. Wang, M.; Li, M.; Xu, L.; Wang, L.; Ju, Z.; Lia, G.; Qiana, Y. *Catal. Sci. Technol.* **2011**, *1*, 1159.
23. Ameen, S.; Seo, H. K.; Akhtar, M. S.; Shin, H. S. *Chem. Eng. J.* **2012**, *210*, 220.
24. Raza, W.; Haque, M. M.; Muneer, M.; Fleisch, M.; Hakki, A.; Bahnemann, D. *J. Alloys Compd.* **2015**, *632*, 837.
25. Shen, F.; Que, W.; He, Y.; Yuan, Y.; Yin, X.; Wang, G. *ACS Appl. Mater. Interfaces* **2012**, *4*, 4087.
26. Leven, I.; Azuri, I.; Kronik, L.; Hod, O. *J. Chem. Phys.* **2014**, *140*, 104106.
27. Sultan, A.; Ahmad, S.; Anwer, T.; Mohammad, F. *RSC Adv.* **2015**, *5*, 105980.
28. Anwer, T.; Ansari, M. O.; Mohammad, F. *Polym. Plast. Technol. Eng.* **2013**, *52*, 472.
29. Tang, C. C.; Bando, Y.; Sato, T.; Kurashima, K. *Adv. Mater* **2002**, *14*, 1046.
30. Zhao, Z.; Yang, Z.; Wen, Y.; Wang, Y. *J. Am. Ceram. Soc.* **2011**, *94*, 4496.
31. Ansari, M. O.; Mohammad, F. *J. Appl. Polym. Sci.* **2012**, *124*, 4433.
32. Raza, W.; Haque, M. M.; Muneer, M. *Appl. Surf. Sci.* **2014**, *322*, 215.
33. Yin, H.; Yu, K.; Song, C.; Huang, R.; Zhu, Z. *ACS Appl. Mater. Interfaces* **2014**, *6*, 14851.
34. Bin Mukhlish, M. Z.; Najnin, F.; Rahman, M. M.; Uddin, M. J. *J. Sci. Res.* **2013**, *5*, 301.
35. Raza, W.; Haque, M. M.; Muneer, M.; Harada, T.; Matsumura, M. *J. Alloys Compd.* **2015**, *648*, 641.
36. Wang, C.; Ao, Y.; Wang, P.; Hou, J.; Qian, J. *Powder Technol.* **2011**, *210*, 203.
37. Wu, J.; Coffer, J. L. *J. Phys. Chem. C* **2007**, *111*, 16088.
38. Haque, M. M.; Raza, W.; Khan, A.; Muneer, M. *J. Nanoeng. Nanomanufacturing* **2014**, *4*, 135.
39. Eskizeybek, V.; Sarı, F.; Gülce, H.; Gülce, A.; Avcı, A. *Appl. Catal. B Environ.* **2012**, *119120*, 197.